



HAL
open science

Production of 100% Cellulose Nanofibril Objects Using the Molded Cellulose Process: A Feasibility Study

Fleur Rol, Marie Billot, Marco Bolloli, Davide Beneventi, Julien Bras

► To cite this version:

Fleur Rol, Marie Billot, Marco Bolloli, Davide Beneventi, Julien Bras. Production of 100% Cellulose Nanofibril Objects Using the Molded Cellulose Process: A Feasibility Study. *Industrial and engineering chemistry research*, 2020, 59 (16), pp.7670 - 7679. 10.1021/acs.iecr.9b06127 . hal-03096502

HAL Id: hal-03096502

<https://hal.science/hal-03096502>

Submitted on 9 Aug 2022

HAL is a multi-disciplinary open access archive for the deposit and dissemination of scientific research documents, whether they are published or not. The documents may come from teaching and research institutions in France or abroad, or from public or private research centers.

L'archive ouverte pluridisciplinaire **HAL**, est destinée au dépôt et à la diffusion de documents scientifiques de niveau recherche, publiés ou non, émanant des établissements d'enseignement et de recherche français ou étrangers, des laboratoires publics ou privés.

Production of 100% CNF object using the molded cellulose process: a feasibility study

Fleur Rol †, Marie Billot †, Marco Bolloli †, Davide Beneventi †, Julien Bras,†, A*

† Univ. Grenoble Alpes, CNRS, Grenoble INP, LGP2, F-38000 Grenoble, France

Λ Institut Universitaire de France (IUF), F-75000 Paris, France

E-mail address

Fleur.rol@lgp2.grenoble-inp.fr

Marie.billot@grenoble-inp.fr

Marco.bolloli@grenoble-inp.fr

davide.beneventi@grenoble-inp.fr

Julien.bras@grenoble-inp.fr

KEYWORDS. nanocellulose, 3D printing, molded nanocellulose

ABSTRACT. Vacuum-assisted light compression molding was used to produce 3D objects by shaping cellulose nanofibrils pastes in order to overcome the lack of mechanical resistance and barrier properties of objects made by molding conventional papermaking fibers. This well-known industrial process, currently used for the production of low-end cellulose packaging, was simulated by using 3D-printed polycarbonate porous molds both during the vacuum-assisted dewatering and the heat compression stages. High solid content cellulose nanofibril (CNF) pastes produced by twin screw extrusion (TSE) were used as base material and different methods were used to form the cellulosic mats and to dry the obtained 3D object. Different drying techniques were tested in order to produce a transparent object and minimize shrinkage upon drying, i.e. oven, thermo-press, microwaves, freeze drying or a combination. Nevertheless, as a consequence of the important shrinkage of CNF during the drying step and of the high residual porosity in the final dry material, none of the techniques yielded transparent and dimensionally stable 3D objects.

INTRODUCTION

Today oligomers derived from petrol are used in many applications and to produce both low-end and technical thermoplastic materials. Nevertheless, the use of these plastics is strongly questioned by the depletion of oil resources or pollutions issues and the industrial production is progressively converting the use of sustainable and renewable raw materials. Cellulose is one of the most important bio-based polymer and is already used in industries such as paper making.¹

Native cellulose is not a thermoplastic polymer, it is not fusible and it cannot be used in traditional converting processes used in plastic industries such as thermoforming or injection molding. Only when mixed with a thermoplastic polymer as reinforcing element cellulose-based composites can be formed using those processes. Paper and textile are the main cellulose application. Cellulose can also be processed by dissolution/regeneration such as Lyocell process and hence formed regenerated fibers or all cellulose composites²⁻⁶ made of a matrix of dissolved cellulose reinforced with untouched fibers. Cellulose can also be hot pressed to produce 3D object without the use of chemical or binder.⁷⁻⁹

Another method to produce 100% cellulosic object is the molded cellulose process. Used to produce eggs box or wedging elements since about 100 years, this process is now more and more used to produce high quality products such as disposable dishes or meal trays. This process is based on proprietary industrial know-how and empiricism and it has been poorly investigated. Most of the time, cellulose fiber suspensions with a low dry content are retained on a porous metallic mold by vacuum-filtration and then dried in a mold under pressure or not. Historically used for cheap applications using low-quality recycled fibers as raw material, today this process is also used to produce high value added products made of bleached cellulosic fibers. However, the molded cellulosic objects present still poor mechanical properties and low barrier properties which limit their field of application.

Several years ago, types of cellulose nanoparticles with high mechanical properties and high barrier properties have been developed and generally labeled as nanocelluloses. Two main types of nanocelluloses can be produced from the cellulosic fibers: cellulose nanocrystals (CNC) and cellulose nanofibrils (CNF). CNC are produced via an acid hydrolysis of the cellulose fibers and are characterized by a high crystallinity and a rigid-like morphology. CNF are produced via a chemical/enzymatical¹⁰⁻¹² treatment of cellulose fibers followed by a mechanical process¹³⁻¹⁷ as recently reviewed by Rol et al.¹⁸. Those CNF present high mechanical properties^{12,13,19,20}, high grease, oxygen and water vapor barrier properties^{21,22} and the films produced are transparent.^{23,24} For now, CNF suspensions are

produced at really low solid content, namely between 2 and 5 wt% which limits their field of application. Moreover, they present a gel-like behavior and really high viscosity²⁵ which make their filtration difficult. Since few years, CNF can be produced at high solid content, namely 20 wt% or more using a twin screw extruder (TSE).^{20,26,27} These concentrated CNF suspensions present 10 times less water which reduces the transport cost but also widen the field of application of CNF.

It is known that the water associated to the fibers can be of different forms: free water, freezing bounded water and non-freezing bounded water.²⁸ Freezing bounded water is water linked to the OH groups of the hydrophilic cellulose fibers and non-freezing bounded water is a subset of bounded water. The free water is trapped in interstices or capillaries and constitutes the majority of the water in a cellulosic fibers suspension. Free water can be easily removed contrary to the others. The drainage rate is always decreased when cellulosic fibers are nanofibrillated¹⁴ as previously reported for fines and refined fibers.²⁹ Indeed, CNF have a high specific surface area and high aspect ratio which leads to the formation of a strong cross-linked network and pseudoplastic behavior even at 2 wt% dry content.^{30,31} The drainage time increases with the increase CNF content but also with the CNF quality, i.e. when the size decreases.^{14,32,33} CNF possess higher number of available OH groups than fibers and the bounded water amount increases.³⁴⁻³⁶ The high solid content CNF were recently developed and for now there is no study on the water drainage in this concentrated suspension. High solid content CNF maybe contained more bounded water more difficult to remove. However, they do have the advantage that it can be directly pressed. Moreover, drying is really complex field and different forces such as capillary or diffusion forces can occur. Agglomerations and drying mechanisms are dependent on the particular drying method.³⁷ For now, CNF can be dried using various techniques such as oven drying, freeze drying, supercritical extraction or spray drying as recently reviewed.³⁸ However, the formation of nanocellulosic films or objects is still challenging. CNF films shrink a lot during the drying due to faster water evaporation at the surface than within the material³⁹ and due to moisture gradient in the cellulosic object.

The aim of this study is to take advantages of the high solid content CNF to try to produce 3D object made of 100% CNF by adapting the cellulose molding process. Due to the high consistency, CNF mats can be formed rapidly, hot pressed and dried. Up to our knowledge, there is no study reporting the production of 3D CNF objects using the cellulose molding process. The objective of this study was then to produce a 3D object, mechanically resistant with barrier properties and made of 100% CNF. The molding cellulose process was simulated

using a 3D printed polycarbonate mold, a vacuum pump and a hot press. Indeed, for now, the metallic molds used in the molded cellulose industry are expensive, difficult to produce and cannot present complicated forms. 3D printing was identified as a cheap, rapid and easily feasible process to produce porous molds useful to simulate the cellulose molding process. Molds with different filling degree and porosities were hence produced and characterized. Different raw materials, different methods to form the cellulosic mats and different drying methods were then tested to try to form 3D CNF objects.

MATERIAL & METHODS

Materials

Cellulose used throughout this work is eucalyptus bleached kraft pulp from Fibria, Brazil. The chemicals were used as received: FiberCare[®] enzymes solution from Novozymes, Sodium acetate trihydrate (Sigma, >99%), Acetic acid (Sigma, >99%) and polycarbonate filaments for 3D printing. Distilled water was used in all suspensions and solutions preparation.

Methods

3D printing. A SpiderBot 3D printer from Qualup SAS (France), equipped with an heated chamber and an additional bed heating resistance was used to print the filtration mold in polycarbonate (Addifrance). The design of the mold was done thanks to the software Autodesk 123D design. The nozzle diameter was 0.5 mm, the average velocity fixed at 50 mm/s and the layer thickness 200 μm . The printing temperature of the extruder hot end, the printing bed and the print chamber were set to 295°C, 150°C and 65°C, respectively. In order to control the mold porosity, the filtration mold was printed without solid perimeter walls and using a rectilinear infill (with a volumetric infill ratio ranging between 35 and 75%) with cross angle between successive layers of 90°deg. The mold is presented in the following part. The time to produce a mold was between 3 and 10 hours. The surface porosity of the flat and curved part of the mold was estimated using test specimens 3D printed using different filling degrees and with the normal of the planar reference surface inclined from 0 to 90°deg with respect to the normal of the print bed. The references surfaces were imaged by optical microscopy and their open porosity was determined by image analysis (Image J software).

Mechanical property of the polymer mold. Samples of different porosities were printed to evaluate the tensile strength properties of the mold depending on its filling degree. The specimen were tested using an Instron 5965 machine equipped with a load cell of 5 kN

capacity at a cross-head speed of 2 mm/min. Specimen with a size of 7 x 1 cm and a thickness of 5 mm were tested. At least five specimens were tested for each sample and average is presented.

Production of CNF by twin screw extrusion (TSE). Refined cellulose fibers at 2 wt% were enzymatically hydrolyzed using 300 ECU/g of cellulose of cellulase Fiber Care® from Novozymes. The treatment was done at pH 5 for 2 h at 50°C. First, pH was adjusted using a buffer of sodium acetate trihydrate and acetic acid. After 2h, the temperature was increased at 85 °C and let 15 min. Cellulose fibers were then washed with distilled water under filtration and filtered until a dry content of 20 wt%. CNF were then produced using a twin screw extruder (Model Thermoscientific HAAKE Rheomex OS PTW16 + HAAKE PolyLab OS Rheodrive 7) with an L/d ratio of 40 as reported in a previous study.²⁰ The speed was set at 400 rpm and the temperature maintained close to 10°C.

Process to produce molded nanostructured object

The molded nanostructured objects were produced following 3 steps.

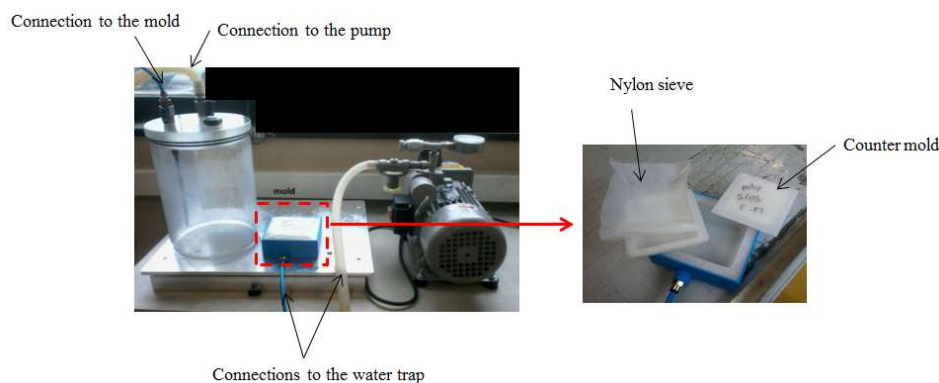


Figure 1. Protocol used to simulate the filtration and aspiration step of the molded cellulose process.

Step 1: Formation of the cellulose mat by filtration by gravity or under vacuum aspiration. The filtration part of the mold produced by 3D printing was covered with a nylon sieve with a mesh size of 1 μm to avoid clogging. Cellulose suspensions and CNF suspensions at different dry content (namely 2 wt% or 20 wt%) were placed in the mold and covered with the backing mold as represented in Figure 1. The mold was connected or not to a pump. Filtration was done by gravity or with the pump (-0.5 bar) and the dry content of the formed cellulosic mat was measured at different time.

Step 2: Formation of the cellulosic mat using a press. Cellulose fibers and CNF at high dry content were placed between the mold equipped with a nylon sieve and the backing mold and

pressed under different pressure from 0 to 10 MPa for 1 min. Different equipments were used: a hot press, Saint Eloi with a maximum load of 200 kN at ambient temperature or a manual press (Specac, Eurolabo, Paris) with a maximum load of 15 tons at ambient temperature.

Step 3: Process to dry the produced object. The cellulosic mats formed using one of the previous described techniques were dried using different strategies. The drying was done inside the mold with the backing mold.

Oven. The cellulosic mat formed in the mold was placed into an oven at 110 °C and loaded with a 300 g of metallic weight to limit the shrinking. Evolution of the dry content with the time was followed.

Hot press. The formed cellulosic mats were dried in the hot press described in the previous part. After being pressed at 4 tons for 1 min using the manual press, samples were dried for different times in the hot press at 110 °C with a pressure of 4 MPa. The evolution of the dry content was followed.

Microwaves. A kitchen microwave with a maximal power of 700 W was used to dry 3D object. First, the complete mold was encircled with elastics to avoid dimensional deformation. The mold was then elevated in the microwaves to facilitate air circulation and water evaporation. Different powers (480 or 560W) and times (0 to 4 min) were used. After each minute, the microwave was opened to eliminate the created water vapor.

Freeze dryer. The mold containing the 3D object was frozen in a freezer at -12°C for 24h and then freeze dried using a ALPHA 2-4 LD plus, Christ LCG freeze dryer for 2 days.

Characterizations techniques of CNF

Optical microscopy. The porosity of the designed molds was observed using optical microscope (Carl Zeiss Axio Imager M1) equipped with an AxioCam MRc 5 digital camera. At least, ten pictures were done and the most representatives were selected. The size of the pores was hence measured using ImageJ software and a minimum of 20 measurements were done. The same equipment was used to observe CNF suspension morphology. CNF suspensions were diluted to 0.5 wt% using an Ultra-Turrax and images were taken. The most representatives are shown.

Atomic force microscopy (AFM). CNF suspensions were diluted to 10⁻² wt% using an Ultra-Turrax. One drop was deposited on a mica disk and dried overnight at ambient temperature. AFM was performed in a scan assist mode using Dimension Icon Atomic Force Microscope

with an OTESPA cantilever. A minimum of 5 areas was scanned for each sample and the most representative images are shown.

Transmission electron microscopy (TEM). TEM analysis was done using a transmission electron microscope (FEI/Philips CM 200) with an accelerating voltage of 200 kV equipped with a camera (TemCam F216, TVIPS). CNF suspensions were diluted to 10⁻³ wt% and dropped on copper grids covered with amorphous carbon.

Formation of Nanopapers and CNF casted film. Nanopapers of 60 g/m² were formed by diluting CNF suspension followed by a filtration through a standard sheet former (Rapid Kothen, ISO 5269-2 standard). The sheet former was equipped with a nylon sieve with a mesh size of 1 μm. Nanopapers were then dried under vacuum for 20 min at 90°C. Casted CNF films were produced by casting 50 mL of the CNF suspension diluted to 0.5 wt% in plastic Petri box. The films of 45 g/m² were dried in a conditioned room at 23 °C and 50% RH for 7 days.

Quality index. CNF suspension quality was evaluated using the quality index developed by Desmaisons et al.⁴⁰. In this study, the simplified version was used and QI* was calculated as below:

$$QI^* = 0.3x_1 - 0.03x_2 - 0.072x_3^2 + 2.54 x_3 - 5.34\ln(x_4) + 58.62$$

where x₁= nanosized fraction [%]; x₂= turbidity [NTU]; x₃= Young's modulus [GPa] of the CNF nanopaper; x₄= macro size [μm²] measured using Image J software and optical microscopy images.

Nanosized fraction. CNF suspensions is diluted using an Ultra-Turrax until a concentration of 0.02 wt% and then centrifuge for 15 min at 1,000g using a centrifuge (Sigma 3-18 KS, Germany). The nanosized fraction⁴¹ of the CNF suspension corresponds to the concentration of the suspension after centrifugation divided by the concentration of the suspension before centrifugation.

Turbidity. The turbidity of diluted CNF suspension at 0.1 wt% was measured using a portable turbidimeter (AL 250 T-IT), with a range between 0.01 and 1,100 NTU. A minimum of ten measurements were done and averages were calculated.

Mechanical properties. An Instron 5965 machine equipped with a load cell of 5 kN capacity was used to measure the Young's modulus of CNF nanopaper of 60 g/m². Mechanical properties were tested on rectangular specimen with dimension of 100 x 15 mm at a cross-head speed of 10 mm/min.

Transparency. The transparency of casted films was measured using an Haze meter (BYK Gardner, Haze-Gard Plus) according to the standard NF T 54-111, 1971. For each film, a minimum of 5 tests were performed and the average is presented.

Characterizations techniques of produced object

Solid dry content measurement. The solid dry content of the cellulosic mat formed was measured using classical method. Difference was made between the mat formed in the walls of the mold or at the bottom.

Mechanical properties of cellulose materials. Young's modulus of the produced object was measured using an Instron 5965 machine equipped with a load cell of 5 kN. First samples were cut at 40 mm long and 10 mm width and then tested at a cross head speed of 2 mm/min. At least 3 tests were done per conditions.

Grease barrier. Grease resistance of the samples was tested according to standard TAPPI T-507. Blotting paper of 6.1 x 6.1 cm² was impregnated with commercial oil colored with Sudan III red dye and placed on contact with the produced sample previously cut in 8 x 8 cm² square. Another fresh blotting paper was placed on the other side of the sample to replicate the penetrated oil. The sandwich was placed between two pieces of aluminium and put in an oven at 60°C for 4h covered with a weight of 365 g. After 4h, the presence of oil on the fresh blotter paper was checked and visually evaluated.

Water Vapor Transmission Rate (WVTR). WVTR of the produced samples were estimated by gravimetric method according to the standard TAPPI T 464 om-12. Tests were monitored at 23 °C and 50% RH. The weight-uptake of anhydrous CaCl₂ in a metal cup covered by the sample was measured. The sample surfaces were reduced to 5.3 cm² using impermeable aluminium scotch and used as top of metal cup. Measurements were done at least 3 times and the average is presented.

RESULTS & DISCUSSIONS

The main objective of this study was to produce transparent 3D objects, made of 100% CNF by adapting the process used for production of molded cellulose.

3D printing was used to produce the filtration mold and simulate the metallic grids used in the cellulose molded industry. First a mold was 3D printed and then molded objects were produced.

Characterization of the CNF used

Two types of CNF were used through this work: (i) a commercial CNF grade produced by an enzymatic pretreatment and using an homogenizer at 2 wt% solid content and (ii) high solid content CNF (20 wt% solid content) produced by enzymatic hydrolysis of cellulose fibers and twin screw extrusion. Both CNF suspensions were then characterized using several techniques. Morphologies of CNF suspensions at different scales are shown in Figure 2. Both CNF suspensions present nanosized fibers and casted films are transparent.

The quality of the CNF suspensions were evaluated using the simplified quality index (QI*) developed by Desmaisons et al.⁴⁰ The results are shown in Table 1. Both CNF suspensions at 2 and 20 wt% present high QI* in accordance with the one reported for commercial CNF.

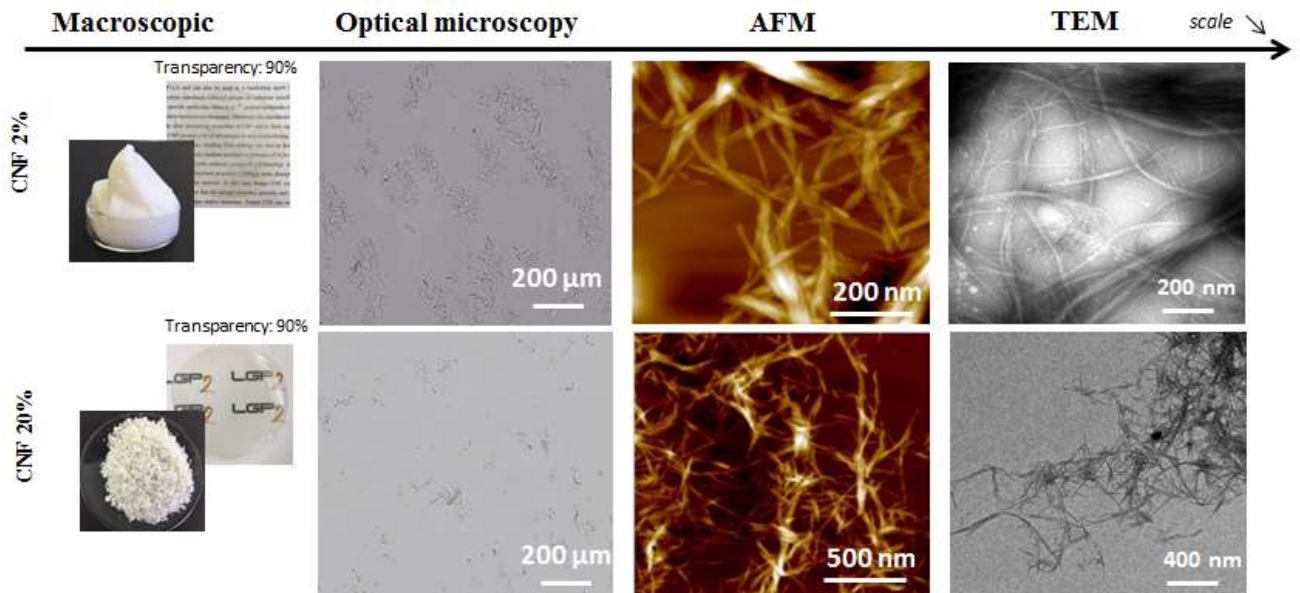


Figure 2. Characterizations of CNF produced by TSE.

Table 1. Simplified Quality Index of the CNF suspensions used throughout this work.

	Macro length [μm^2]	Nanosized fraction [%]	Turbidity [NTU]	Young's modulus [GPa]	QI*
CNF 2%	27.3 ± 8.1	73.2 ± 14.6	413 ± 47	11.8 ± 3.2	70 ± 5.8
CNF 20%	40.6 ± 11.5	64.3 ± 9.9	289.1 ± 13.4	11.6 ± 0.3	69.5 ± 1.8

Production of the filtration mold by 3D printing

A mold representing a tray was designed as reported in Figure 3. The idea was to check both plane and curved parts. The mold is divided in four parts in order to be able to reproduce quickly the possible broken parts and to make several changes regarding the filtering part without printing again the entire mold. The mold has a dimension of 110 x 110 x 40 mm but the efficient filtering part (part (b)) was designed with dimension of around 80 x 80 x 30 mm. The most important part is part (b). This part will monitor and limit the filtration. It has been designed with different degree of filling, namely 35, 50 and 75% full (or 65, 50 and 25% of empty). Part (a) was designed with low porosity (75% filled) to be more resistant and closed in order to limit the CNF penetration. It will be not changed insofar as it is not used during the filtration process. Parts (c) and (d) were printed with high porosity to allow an easier evacuation of the water. It will not influence the filtration step insofar as part (b) is the limiting part of the filtration.

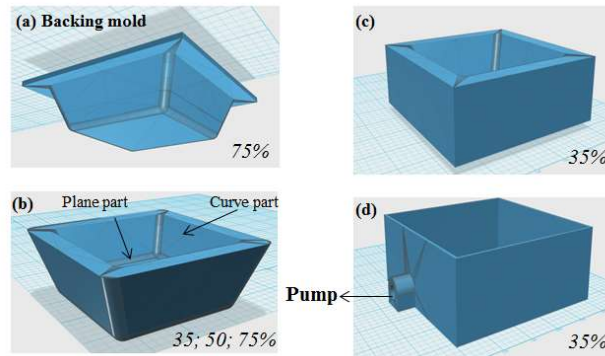


Figure 3. 3D printed mold designed on four parts to simulate the cellulose molding process.

Different porosities will be tested for the part (b) to increase the efficiency of the water evacuation without degrading the mechanical resistance of the mold. The different tested porosities were evaluated measuring the pore sizes of the mold by optical microscopy as reported in Figure 4a. Some pores are clogged by the CNF suspension, especially in the mold of 35% filling degree.

As expected, molds porosity decreased when increasing the filling degree. An average pore surface of 0.5, 0.2 and 0.06 mm² was measured on the plane part of the mold with filling degree of 35, 50 and 75%, respectively.

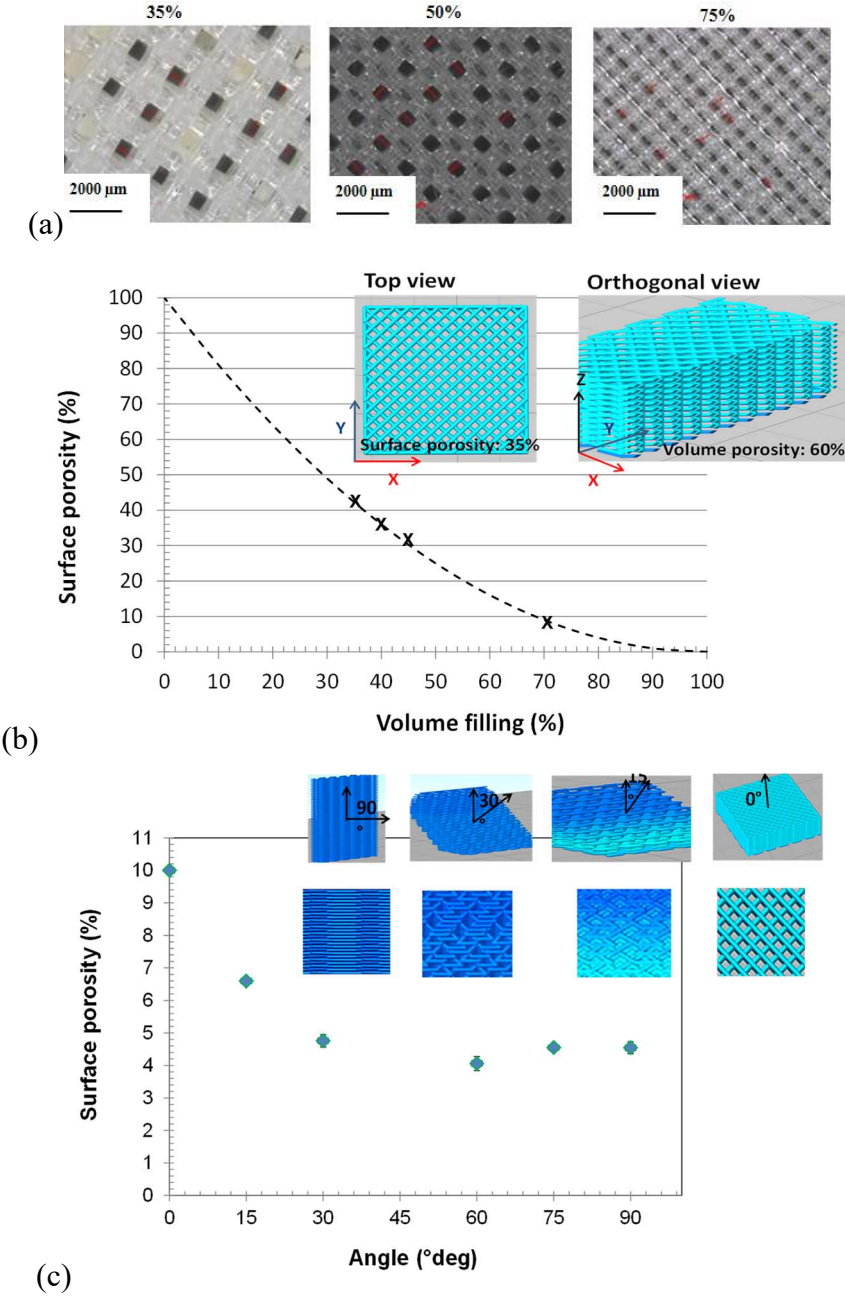


Figure 4. (a) Optical images of the produced molds printed with different filling degrees. (b) Variation of the surface porosity of the plane mold part plotted as a function of the volume filling. Dotted line represents the theoretical surface porosity vs. volume filling as obtained from simple geometrical correlations and x represents experimental surface porosity data obtained from image analysis. (c) Plot of the surface porosity as a function of the mold surface angle with respect to the normal to the print bed.

In some cases, the dimension of the pores was up to three orders of magnitude larger than the nanofibers size that is why the mold was equipped with a nylon sieve with a mesh size of 1 μm before mat forming. Figure 4b shows that the measured surface porosity (i.e. the ratio between the open to the total surface) is lower than the volume porosity. Indeed, samples with 30, 55, 60 and 65% volume porosity had surface porosity of 9, 30, 40 and 35%, respectively. This difference was due to the used linear infill pattern, where the mesh is generated by alternating one layer of parallel filaments along one direction to another with filaments perpendicular to those in the layer below (see inset in Figure 4b). Moreover, owing to the layer by layer filament deposition typical of 3D printing, mold surface porosity was affected by its orientation with respect to the normal to the print bed. Figure 4c shows that the mold surface porosity with 70 filling linearly decreased from 9 to ca. 4% when the surface angle was increased from 0 to ca. 35°deg. Above this angle the progressive variation in the surface structure had not effect on the surface porosity determined by image analysis. Whatever the filling degree and mold surface orientation, the pores repartition in the flat and curved parts was regular which reflected a good 3D printing and led to presage a homogeneous filtration.

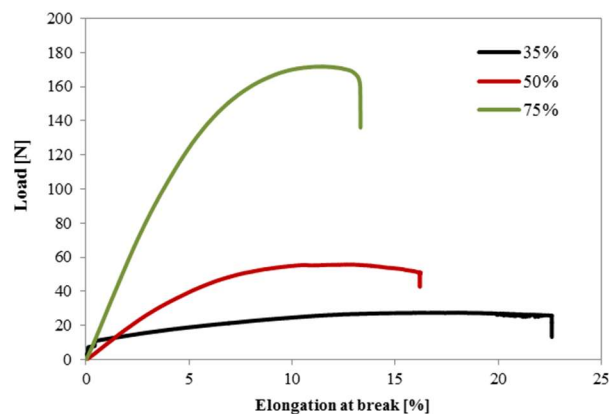


Figure 5. Mechanical resistance of 3D printed objects depending on their filling degree.

In order to identify the best compromise between mold mechanical resistance and dewatering performance, different parts of the mold were then gathered together, covered with a nylon sieve of 1 μm and filtration tests were done with cellulose fiber suspension by varying the porosity of the part (b). The water removal efficiency of the different molds in both the plane and the curved parts was tested and reported in Figure 6. The dewatering efficiency was evaluated measuring the dry content of the cellulosic mats after different time of vacuum-assisted (-0.5 bars) filtration using cellulosic fibers suspension with a dry content of 2 wt%. It is worth noting that the external part of the mold was obstructed with parafilm in

order to avoid air leaking and to attain a constant suction vacuum. Figure 6 shows that, for all tested conditions, when the filling degree increases, subsequently inducing a decrease in the mold surface porosity, the water removal kinetics slows down. Fiber mats formed in the curved zone systematically displayed a dry content lower than those formed in the plane zone of the mold. This difference was associated to the surface porosity of the curved/inclined zone, which was generated by layer stacking during 3D printing, had irregular pores with one constant dimension of 200 μm and was systematically lower than that of the plane zone, which was generated by the regular mesh shown in Figure 4.

A filling degree of 75% provided molds with the highest mechanical resistance while maintaining sufficient porosity for water and steam permeation during dewatering and drying, however the fastest dewatering kinetics was provided by low resistance molds with a filling degree of 35%. In order to maximize water removal from CNF pastes during the molding process, a filling degree of 35% was selected. Finally, a difference of about 2 wt% was observed comparing the dry content of the cellulose mat formed in the plane or in the curved part. This difference in the dry content will probably influence the formation of stable 3D object. To conclude, a modular mold in four parts (Figure 3) was 3D printed using a filling degree of 35% for the filtering part and 75% for the backing mold. Different methods will be tested to form continuous cellulose nanofibers mats.

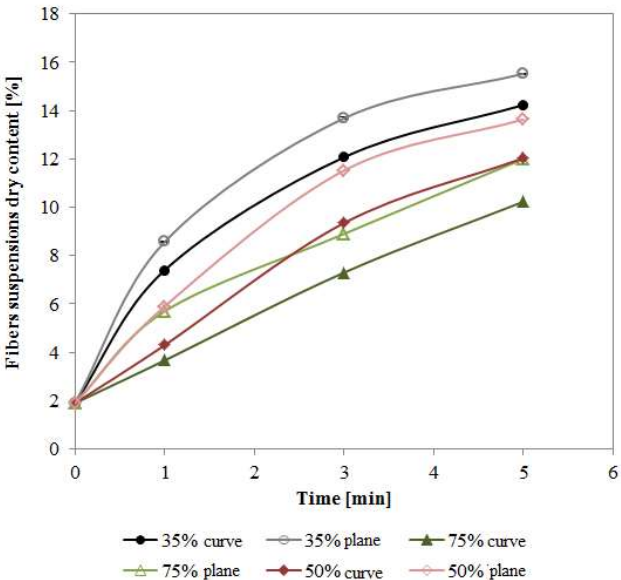


Figure 6. Evacuation of water of the cellulose fiber suspension by aspiration using the different printed molds for the plane part and the curve part of the mold.

Formation of 3D cellulosic objects: filtration (Step 1) and pressing (Step 2)

CNF-fiber mats were formed according to three different methods: (i) filtration by gravity, (ii) filtration by aspiration as reported in Figure 1 and (iii) use of a manual hydraulic press.

As reported in Figure 7, using only gravity, does not allow increasing the dry content of CNF suspensions whatever their concentration due to the low amount of free water. Only the dry content of the cellulose fibers suspensions at 2 wt%, refined or not, was increased from 2 wt% to a stabilized dry content of around 10 wt%. In a cellulosic suspension at 10 wt% dry content whatever the size of the fibers, the water is trapped into the fibers network, the path to remove water is more tortuous and water cannot be removed by gravity.

The mold was then connected to a vacuum pump to filter with aspiration (-0.5 bar) and then to increase the water removal. Unfortunately the aspiration does not allow to increase the dry content of the cellulosic mats formed except for cellulose suspension, refined or not, with a dry content of 2 wt%. The aspiration was not sufficient to filter CNF at 2 wt% due to their viscous and gel-like behavior.²⁵ Water is linked to cellulose and trapped into fibers network and the vacuum applied is not enough. The final stabilized dry content obtained for non-refined cellulose fibers at 2 wt% is higher than the one obtained for refined fibers suspension with a same concentration. Indeed, refining creates fines which decrease the porosity of the cellulosic mats and thus decrease the efficiency of the filtration.

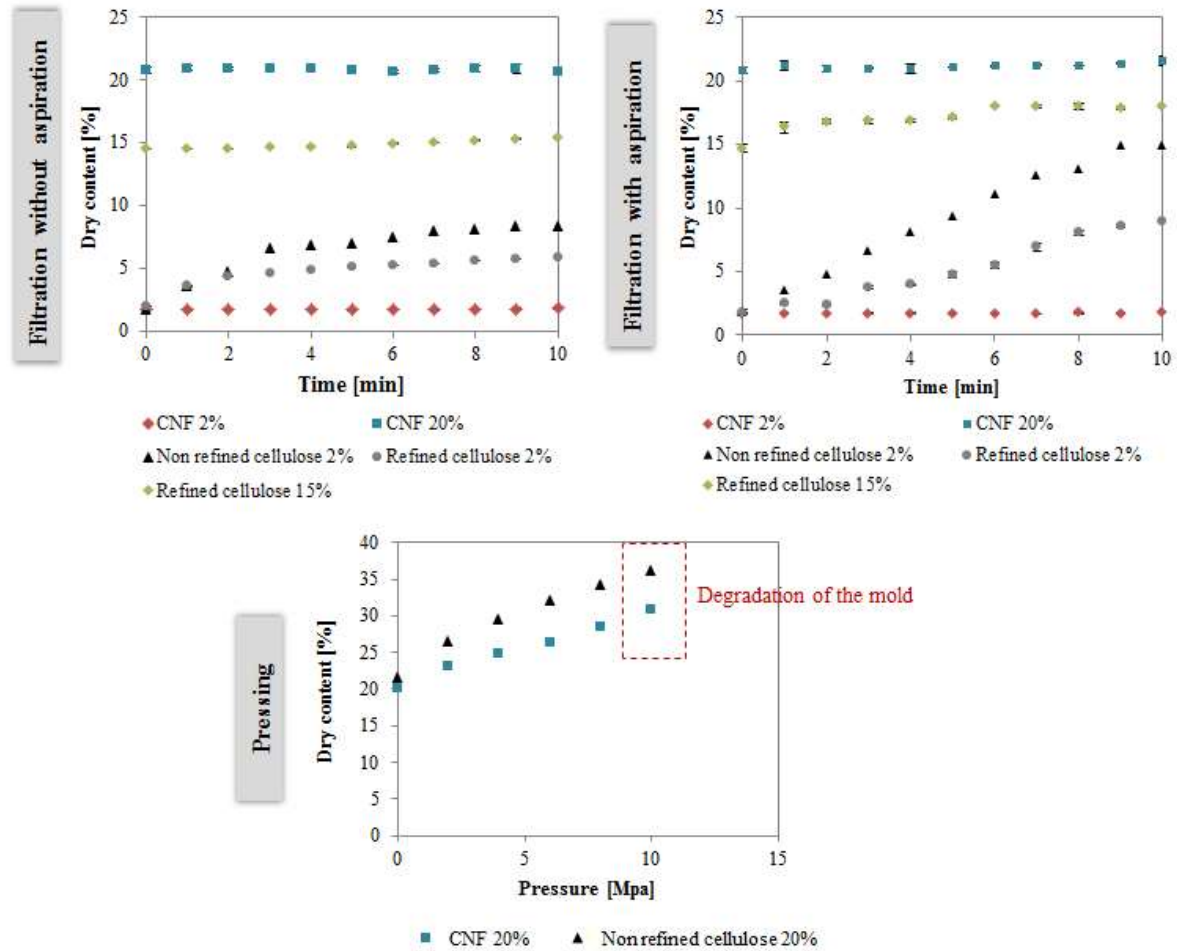


Figure 7. Dry content of the CNF mat formed in the mold plane part filtration (step 1) and pressing (step 2).

The 2nd step method tested to form a nanocellulosic mat is the pressing using a manual hydraulic press. Only the cellulose suspension with a dry content of 20 wt% has been tested whatever the fibers size because a too diluted suspension, with high content of free water, will lead to leaks and cannot be pressed. The combination of aspiration and pressing was not tested.

Increasing the pressure allows to evacuate water of high solid content cellulose fibers or nanofibers suspensions and to reach a dry content of around 30-35 wt%. Higher dry content are obtained for cellulose fibers due to lower bounds between cellulose and water due to lower specific area and so amount of H-bonds. Moreover, cellulose mat made of fibers is more porous due to fiber size and let the water pass more easily. However, experiments were stopped after 10 MPa because a too high pressure degrades the mold. 10 MPa is much higher than the data reported in Figure 5 but the tensile tests were done on small and thin test tubes in order to see the evolution of mechanical properties with the filling degree. Furthermore, at 6

MPa, the cellulosic mats formed in the mold start to break, especially in the connecting parts between the plane and the curved parts of the mold. Khakalo et al.⁴² reported the same phenomenon when hot pressing special paper.⁴² To conclude, a maximal pressure of 4 MPa should not be exceeded.

Finally, a continuous cellulose mats made of high solid content CNF can be formed by pressing at 6 MPa and the maximal dry content reached is 30 wt%. Thanks to the production of high solid content CNF, 100% CNF mats can be produced and manipulated whereas it will required many hours of filtration and or pressing with classic CNF suspension. As shown in Figure 7, increasing the concentration of CNF suspension starting from a 2 wt% solid content suspension is complicated. CNF suspension at 2 wt% presents a gel-like behavior which makes the evacuation of water complicated by aspiration or by pressing.

Different drying techniques were then tested to formed dry 3D 100% CNF objects.

Drying by different methods (Step 3)

Four different drying methods were tested as reported in Figure 8 and combinations of some of them were also tested as reported in Table 2. As explained in the introduction part, drying is a really complex field.

All the tested methods allow obtaining dry objects but depending on the method, different drying times are required. The quickest method which allows to reach 80-90 wt% dry content is the use of microwaves (4 min) followed by the hot press (40 min), the oven (200 min) and finally the freeze-drier (24 h). However, the use of the microwaves should be limited because the water vapor accumulation can damage the mold and the cellulose mat. Indeed, brown spots are observed on the dry mat after only 2 min at 560 W. However, none of the technique tested allows producing dimensionally stable 3D objects, without fracture or shrinking. Only freeze drying allows maintaining the form of the mold but freeze drying cannot be considered for an industrial application.

Samples present a lot of fractures and shrinking especially in the curved part. This can be due to the higher water content at the beginning of the drying but mainly and to the absence or lower pressure in those areas. Indeed, the backing mold transfers almost all the applied force on the plane part. A too high pressure in the connecting part will also make the mat thinner in those parts and thus more sensitive to failures during the drying. A lot of dimensional instability occurs and the dimension of the object is considerably reduced with the drying which is characteristic of the CNF unrestrained drying.⁴³

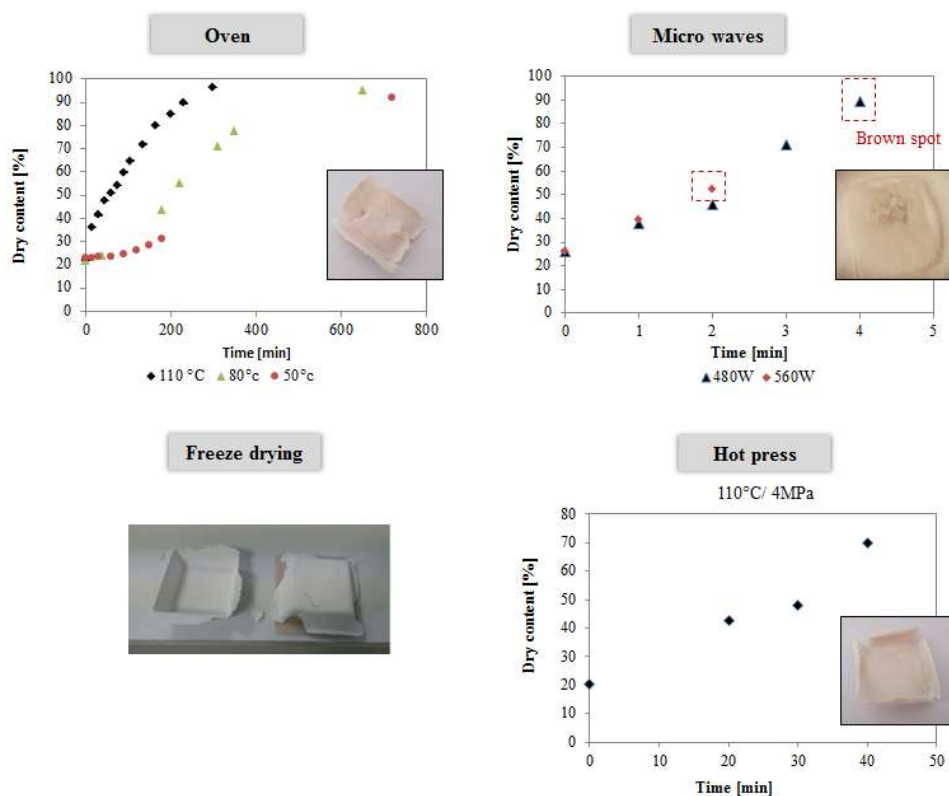


Figure 8. Different methods used to dry the nanocellulosic mats made in the 3D printed mold.

In order to shorten the drying time, combinations of the different processes were also tested as reported in Table 2. Combinations of drying methods were tested on cellulose mats made of fiber or nanofibers. Cellulosic fibers or nanofibers suspensions at 20 wt% were first manually pressed at 4 tons during 1 min and then dried.

Unfortunately, none of the combinations allow obtaining 3D object with stable and maintained dimensions but the time to reach the same final dry content is decreased and does not exceed 2 h whereas a maximum of around 6 h was required to dry the sample with the oven. The combination of different drying processes decreases the drying time but required two processes which can be a limit regarding the production at industrial scale. However, the combination #4 does not allow reaching sufficient dry content when CNF are used. Finally, no difference was observed on the visual appearance of the produced molded object.

Table 2. Combination of different drying methods to produced 3D object.

#	Process 1			Process 2			Total time of drying [min]
	Process	Dry content reached for CNF [%]	Dry content reached for non-refined fibers [%]	Process	Dry content reached for CNF [%]	Dry content reached for non-refined fibers [%]	
1	Hot press 4MPa, 100°C, 30 min	83	96	Micro waves, 3 min, 420W	89	99	33
2	Micro waves 3 min, 420 W	40	61	Hot press, 4MPa, 100°C, 30 min	99	99	33
3	Hot press 4MPa, 100°C, 30 min	83	96	Oven, 110°C, 1h20	99	99	110
4	Micro waves 3 min, 420 W	40	61	Oven, 110°C, 1h	63	99	63

Different additional methods such as addition of gelatin or solvent exchange with ethanol^{44,45} were tested to try to improve this drying step but without success.

The drying step appears as the limiting step in our process. A nanocellulosic mat can be easily formed using a manual pressing which allows reaching 30 wt% solid content but the drying step and CNF shrinkage represent a bottleneck for the formation of a dimensionally stable 3D.

Evaluation of properties of the obtained cellulosic object

2D cellulosic objects were produced using a plane mold, as shown in Figure 9. Cellulosic objects were obtained using cellulose non-refined fibers suspension and CNF suspension. Cellulosic fibers and nanofibers suspensions at 20 wt% were pressed for 1 min at 4 tons using the manual press and then dried using the conditions detailed in Table 2. Samples produced were stabilized in a conditioned room (25°C, 50%RH) for seven days before characterizations. The dry content of the samples produced with the condition #4 was then equal to 95%.



Figure 9. Mold produced by 3D printing with a filling degree of 35% to produce 2D cellulosic object.

Young's modulus, grease permeability and water vapor permeability of the obtained object were evaluated and reported in Table 3. Characterizations were classified using “+” grade because not enough repetitions were done. Cellulosic objects made of non-refined fibers cannot be totally characterized because the objects were too damaged and too brittle.

Table 3. Properties of 2D objects formed using the molded cellulose process and non-refined cellulose fibers or CNF. “++++” corresponds to high Young's modulus and low WVTR.

#	Young's modulus [GPa]		Grease barrier Presence of grease		WVTR [g/(m ² .day)]	
	CNF	Non-refined fibers	CNF	Non-refined fibers	CNF	Non-refined fibers
1	++++	/	No	Yes	++	+
2	++	/	No	Yes	++++	+
3	+	/	No	Yes	++	+
4	++	/	Yes	/	++	/

The Young's moduli of the object made of CNF are high but some repetitions should be done before concluding.

Whereas samples made of non-refined fibers were not barrier to grease, the samples made of CNF present good barrier properties to the grease, except for the one made according to the conditions #4. In the conditions of drying #4, a combination of microwaves and oven was done. The microwaves create water vapor inside the material and when water is removed, some pores are created. The obtained object is more porous than with other drying method. When the drying by microwaves is followed by thermo-pressing, as in condition #2 the samples is dried under pressure and then the number of final pores are limited. On the contrary when the microwaves are completed by oven drying, sample is dried without pressure and there is shrinking and pores. The obtained object is more porous and so the grease can pass through it.

The water vapor permeability is considerably decreased when the object was made of CNF instead of fibers. Indeed, due to their smaller size, nanofibrils create a network and prevent the permeation of water vapor through the material. WVTR is decreased because water molecules should follow a more tortuous path to go through the material.

Regarding the different drying techniques, it seems that the two first combinations (microwaves and thermo-press) lead to the best properties. Samples are dried under pressure

with the compression steps which limits the shrinking. The use of pressing seems to be a key point in the formation of 3D object using the molded cellulose process.

However, all of these results are just a proof of concepts and much more trials should be done before concluding.

CONCLUSION

The molded cellulose process was tested to produce 100% CNF, 3D, and mechanically resistant objects starting from a new grade of high solid content CNF produced by twin screw extrusion. The filtration mold was produced using a cheap, easy and highly adaptable technique: 3D printing. After optimizing the mold porosity, different methods were used to form the nanocellulosic mats. The amount of bounded water is much higher in CNF than in cellulosic fibers suspension and the maximal dry content reached was only 30 wt%. This nanocellulosic mat was formed by pressing 1 min at 4 tons and this was possible thanks to the high solid content CNF. Indeed several hours will be required to filter classic CNF at 2 wt% until this solid content due to their gel-like behavior.

Finally different drying methods were tested but unfortunately none of them allow producing 3D transparent object. Indeed, there is a lot of shrinking and failures, especially in the zones between the plane and curved areas of the mold. 2D objects were produced using combination of drying method and present interesting properties such as grease barrier properties and good mechanical properties.

This study was a first step and several perspectives can be listed such as the use of additives, the use of industrial molded cellulose process or the use of a mixed composition of CNF and fibers.

ACKNOWLEDGMENT

Institut Carnot Polynat (Grant agreement n° ANR-16-CARN-0025-01), Centre Technique du Papier (Grenoble, France) and LabEx Tec 21 (Grant agreement n° ANR-11-LABX-0030) supported this research. LGP2 is part of the LabEx Tec 21 (Investissements d’Avenir) and PolyNat Carnot Institutes.

REFERENCES

(1) Lindstrom. The Effect of Filler Particle Size on the Dry-Strengthening Effect of Cationic Starch Wet-End Addition. *Nord. Pulp Pap. Res. J.* **1987**, 02 (04), 142–145. <https://doi.org/10.3183/NPPRJ-1987-02-04-p142-145>.

- (2) Duchemin, B.; Le Corre, D.; Leray, N.; Dufresne, A.; Staiger, M. P. All-Cellulose Composites Based on Microfibrillated Cellulose and Filter Paper via a NaOH-Urea Solvent System. *Cellulose* **2016**, *23* (1), 593–609. <https://doi.org/10.1007/s10570-015-0835-4>.
- (3) Duchemin, B. J. C.; Mathew, A. P.; Oksman, K. All-Cellulose Composites by Partial Dissolution in the Ionic Liquid 1-Butyl-3-Methylimidazolium Chloride. *Compos. Part Appl. Sci. Manuf.* **2009**, *40* (12), 2031–2037. <https://doi.org/10.1016/j.compositesa.2009.09.013>.
- (4) Piltonen, P.; Hildebrandt, N. C.; Westerlind, B.; Valkama, J.-P.; Tervahartiala, T.; Illikainen, M. Green and Efficient Method for Preparing All-Cellulose Composites with NaOH/Urea Solvent. *Compos. Sci. Technol.* **2016**, *135*, 153–158. <https://doi.org/10.1016/j.compscitech.2016.09.022>.
- (5) Orelma, H.; Korpela, A.; Kunnari, V.; Harlin, A.; Suurnäkki, A. Improving the Mechanical Properties of CNF Films by NMMO Partial Dissolution with Hot Calender Activation. *Cellulose* **2017**, *24* (4), 1691–1704. <https://doi.org/10.1007/s10570-017-1229-6>.
- (6) Nishino, T.; Arimoto, N. All-Cellulose Composite Prepared by Selective Dissolving of Fiber Surface. *Biomacromolecules* **2007**, *8* (9), 2712–2716. <https://doi.org/10.1021/bm0703416>.
- (7) Pintiaux, T.; Viet, D.; Vandenbossche, V.; Rigal, L.; Rouilly, A. High Pressure Compression-Molding of α -Cellulose and Effects of Operating Conditions. *Materials* **2013**, *6* (6), 2240–2261. <https://doi.org/10.3390/ma6062240>.
- (8) Pintiaux, T.; Viet, D.; Vandenbossche, V.; Rigal, L.; Rouilly, A. Binderless Materials Obtained by Thermo-Compressive Processing of Lignocellulosic Fibers : A Comprehensive Review. *BioResources* **2015**, *10* (1), 1915–1963.
- (9) Vaca-Medina, G.; Jallabert, B.; Viet, D.; Peydecastaing, J.; Rouilly, A. Effect of Temperature on High Pressure Cellulose Compression. *Cellulose* **2013**, *20* (5), 2311–2319. <https://doi.org/10.1007/s10570-013-9999-y>.
- (10) Nechyporchuk, O.; Pignon, F.; Belgacem, M. N. Morphological Properties of Nanofibrillated Cellulose Produced Using Wet Grinding as an Ultimate Fibrillation Process. *J. Mater. Sci.* **2015**, *50* (2), 531–541. <https://doi.org/10.1007/s10853-014-8609-1>.
- (11) Isogai, A.; Saito, T.; Fukuzumi, H. TEMPO-Oxidized Cellulose Nanofibers. *Nanoscale* **2011**, *3* (1), 71–85. <https://doi.org/10.1039/C0NR00583E>.
- (12) Ghanadpour, M.; Carosio, F.; Larsson, P. T.; Wågberg, L. Phosphorylated Cellulose Nanofibrils: A Renewable Nanomaterial for the Preparation of Intrinsically Flame-Retardant

Materials. *Biomacromolecules* **2015**, *16* (10), 3399–3410.
<https://doi.org/10.1021/acs.biomac.5b01117>.

(13) Nair, S. S.; Zhu, J. Y.; Deng, Y.; Ragauskas, A. J. Characterization of Cellulose Nanofibrillation by Micro Grinding. *J. Nanoparticle Res.* **2014**, *16* (4), 2349.
<https://doi.org/10.1007/s11051-014-2349-7>.

(14) Taipale, T.; Österberg, M.; Nykänen, A.; Ruokolainen, J.; Laine, J. Effect of Microfibrillated Cellulose and Fines on the Drainage of Kraft Pulp Suspension and Paper Strength. *Cellulose* **2010**, *17* (5), 1005–1020. <https://doi.org/10.1007/s10570-010-9431-9>.

(15) Bhatnagar, A.; Sain, M. Processing of Cellulose Nanofiber-Reinforced Composites. *J. Reinf. Plast. Compos.* **2005**, *24* (12), 1259–1268. <https://doi.org/10.1177/0731684405049864>.

(16) Deng, S.; Huang, R.; Zhou, M.; Chen, F.; Fu, Q. Hydrophobic Cellulose Films with Excellent Strength and Toughness via Ball Milling Activated Acylation of Microfibrillated Cellulose. *Carbohydr. Polym.* **2016**, *154*, 129–138. <https://doi.org/10.1016/j.carbpol.2016.07.101>.

(17) Kondo, T.; Kose, R.; Naito, H.; Kasai, W. Aqueous Counter Collision Using Paired Water Jets as a Novel Means of Preparing Bio-Nanofibers. *Carbohydr. Polym.* **2014**, *112*, 284–290. <https://doi.org/10.1016/j.carbpol.2014.05.064>.

(18) Rol, F.; Belgacem, M. N.; Gandini, A.; Bras, J. Recent Advances in Surface-Modified Cellulose Nanofibrils. *Prog. Polym. Sci.* **2018**. <https://doi.org/10.1016/j.progpolymsci.2018.09.002>.

(19) Pei, A.; Butchosa, N.; Berglund, L. A.; Zhou, Q. Surface Quaternized Cellulose Nanofibrils with High Water Absorbency and Adsorption Capacity for Anionic Dyes. *Soft Matter* **2013**, *9* (6), 2047. <https://doi.org/10.1039/c2sm27344f>.

(20) Rol, F.; Karakashov, B.; Nechyporchuk, O.; Terrien, M.; Meyer, V.; Dufresne, A.; Belgacem, M. N.; Bras, J. Pilot-Scale Twin Screw Extrusion and Chemical Pretreatment as an Energy-Efficient Method for the Production of Nanofibrillated Cellulose at High Solid Content. *ACS Sustain. Chem. Eng.* **2017**, *5* (8), 6524–6531. <https://doi.org/10.1021/acssuschemeng.7b00630>.

(21) Lavoine, N.; Desloges, I.; Dufresne, A.; Bras, J. Microfibrillated Cellulose – Its Barrier Properties and Applications in Cellulosic Materials: A Review. *Carbohydr. Polym.* **2012**, *90* (2), 735–764. <https://doi.org/10.1016/j.carbpol.2012.05.026>.

(22) Hubbe, M. A.; Ferrer, A.; Tyagi, P.; Yin, Y.; Salas, C.; Pal, L.; Rojas, O. J. Nanocellulose in Thin Films, Coatings, and Plies for Packaging Applications: A Review. *BioResources* **2017**, *12* (1), 2143–2233. <https://doi.org/10.15376/biores.12.1.2143-2233>.

- (23) Iwamoto, S.; Nakagaito, A. N.; Yano, H. Nano-Fibrillation of Pulp Fibers for the Processing of Transparent Nanocomposites. *Appl. Phys. A* **2007**, *89* (2), 461–466. <https://doi.org/10.1007/s00339-007-4175-6>.
- (24) Yano, H.; Sugiyama, J.; Nakagaito, A. N.; Nogi, M.; Matsuura, T.; Hikita, M.; Handa, K. Optically Transparent Composites Reinforced with Networks of Bacterial Nanofibers. *Adv. Mater.* **2005**, *17* (2), 153–155. <https://doi.org/10.1002/adma.200400597>.
- (25) Nechyporchuk, O.; Belgacem, M. N.; Pignon, F. Current Progress in Rheology of Cellulose Nanofibril Suspensions. *Biomacromolecules* **2016**, *17* (7), 2311–2320. <https://doi.org/10.1021/acs.biomac.6b00668>.
- (26) Ho, T. T. T.; Abe, K.; Zimmermann, T.; Yano, H. Nanofibrillation of Pulp Fibers by Twin-Screw Extrusion. *Cellulose* **2014**, *22* (1), 421–433. <https://doi.org/10.1007/s10570-014-0518-6>.
- (27) Baati, R.; Magnin, A.; Boufi, S. High Solid Content Production of Nanofibrillar Cellulose via Continuous Extrusion. *ACS Sustain. Chem. Eng.* **2017**. <https://doi.org/10.1021/acssuschemeng.6b02673>.
- (28) Nakamura, K.; Hatakeyama, T.; Hatakeyama, H. Studies on Bound Water of Cellulose by Differential Scanning Calorimetry. *Text. Res. J.* **1981**, *51* (9), 607–613. <https://doi.org/10.1177/004051758105100909>.
- (29) Lin, T.; Yin, X.; Retulainen, E.; Nazhad, M. M. Effect of Chemical Pulp Fines on Filler Retention and Paper Properties. *Appita J. J. Tech. Assoc. Aust. N. Z. Pulp Pap. Ind.* **2007**, *60* (6), 469–473.
- (30) Turbak, A. F.; Snyder, F. .; Sandberg, K. . Microfibrillated Cellulose, a New Cellulose Product: Properties, Uses, and Commercial Potential. *J Appl Polym Sci Appl Polym Symp U. S.* **1983**, *37*, 815–827.
- (31) Pääkkö, M.; Ankerfors, M.; Kosonen, H.; Nykänen, A.; Ahola, S.; Österberg, M.; Ruokolainen, J.; Laine, J.; Larsson, P. T.; Ikkala, O.; et al. Enzymatic Hydrolysis Combined with Mechanical Shearing and High-Pressure Homogenization for Nanoscale Cellulose Fibrils and Strong Gels. *Biomacromolecules* **2007**, *8* (6), 1934–1941. <https://doi.org/10.1021/bm061215p>.
- (32) Ryu, J. R.; Sim, K.; Youn, H. J. Evaluation of Dewatering of Cellulose Nanofibrils Suspension and Effect of Cationic Polyelectrolyte Addition on Dewatering. *J. Korea Tech. Assoc. Pulp Pap. Ind.* **2014**, *46* (6), 78–86. <https://doi.org/10.7584/ktappi.2014.46.6.078>.

- (33) He, M.; Yang, G.; Cho, B.-U.; Lee, Y. K.; Won, J. M. Effects of Addition Method and Fibrillation Degree of Cellulose Nanofibrils on Furnish Drainability and Paper Properties. *Cellulose* **2017**, *24* (12), 5657–5669. <https://doi.org/10.1007/s10570-017-1495-3>.
- (34) Afra, E.; Yousefi, H.; Hadilam, M. M.; Nishino, T. Comparative Effect of Mechanical Beating and Nanofibrillation of Cellulose on Paper Properties Made from Bagasse and Softwood Pulps. *Carbohydr. Polym.* **2013**, *97* (2), 725–730. <https://doi.org/10.1016/j.carbpol.2013.05.032>.
- (35) Chang, F.; Lee, S.-H.; Toba, K.; Nagatani, A.; Endo, T. Bamboo Nanofiber Preparation by HCW and Grinding Treatment and Its Application for Nanocomposite. *Wood Sci. Technol.* **2012**, *46* (1), 393–403. <https://doi.org/10.1007/s00226-011-0416-0>.
- (36) Sethi, J.; Oksman, K.; Illikainen, M.; Sirviö, J. A. Sonication-Assisted Surface Modification Method to Expedite the Water Removal from Cellulose Nanofibers for Use in Nanopapers and Paper Making. *Carbohydr. Polym.* **2018**, *197*, 92–99. <https://doi.org/10.1016/j.carbpol.2018.05.072>.
- (37) Peng, Y.; Gardner, D. J.; Han, Y. Drying Cellulose Nanofibrils: In Search of a Suitable Method. *Cellulose* **2012**, *19* (1), 91–102. <https://doi.org/10.1007/s10570-011-9630-z>.
- (38) Zimmermann, M. V.; Borsoi, C.; Lavoratti, A.; Zanini, M.; Zattera, A. J.; Santana, R. M. Drying Techniques Applied to Cellulose Nanofibers. *J. Reinf. Plast. Compos.* **2016**, *35* (8), 628–643. <https://doi.org/10.1177/0731684415626286>.
- (39) Gimaker. Influence of Beating and Chemical Additives on Residual Stresses in Paper. *Nord. Pulp Pap. Res. J.* **2011**, *26* (04), 445–451. <https://doi.org/10.3183/NPPRJ-2011-26-04-p445-451>.
- (40) Desmaisons, J.; Boutonnet, E.; Rueff, M.; Dufresne, A.; Bras, J. A New Quality Index for Benchmarking of Different Cellulose Nanofibrils. *Carbohydr. Polym.* **2017**, *174*, 318–329. <https://doi.org/10.1016/j.carbpol.2017.06.032>.
- (41) Naderi, A.; Lindström, T.; Sundström, J. Repeated Homogenization, a Route for Decreasing the Energy Consumption in the Manufacturing Process of Carboxymethylated Nanofibrillated Cellulose? *Cellulose* **2015**, *22* (2), 1147–1157. <https://doi.org/10.1007/s10570-015-0576-4>.
- (42) Khakalo, A.; Filpponen, I.; Johansson, L.-S.; Vishtal, A.; Lokanathan, A. R.; Rojas, O. J.; Laine, J. Using Gelatin Protein to Facilitate Paper Thermoformability. *React. Funct. Polym.* **2014**, *85*, 175–184. <https://doi.org/10.1016/j.reactfunctpolym.2014.09.024>.
- (43) Ketola, A. E.; Strand, A.; Sundberg, A.; Kouko, J.; Oksanen, A.; Salminen, K.; Fu, S.; Retulainen, E. Effect of Micro- and Nanofibrillated Cellulose on the Drying Shrinkage, Extensibility,

and Strength of Fibre Networks. *BioResources* **2018**, *13* (3), 5319–5342. <https://doi.org/10.15376/biores.13.3.5319-5342>.

(44) Håkansson, K. M. O.; Henriksson, I. C.; Vázquez, C. de la P.; Kuzmenko, V.; Markstedt, K.; Enoksson, P.; Gatenholm, P. Solidification of 3D Printed Nanofibril Hydrogels into Functional 3D Cellulose Structures. *Adv. Mater. Technol.* **2016**, *1* (7), 1600096. <https://doi.org/10.1002/admt.201600096>.

(45) Pras, O.; Beneventi, D.; Chaussy, D.; Piette, P.; Tapin-Lingua, S. Use of Microfibrillated Cellulose and Dendritic Copper for the Elaboration of Conductive Films from Water- and Ethanol-Based Dispersions. *J. Mater. Sci.* **2013**, *48* (20), 6911–6920. <https://doi.org/10.1007/s10853-013-7496-1>.